

Transfer matrix approach to quantum conductivity calculations in single-wall carbon nanotubes

Antonios N. Andriotis^{a)}

Institute of Electronic Structure and Laser, Foundation for Research and Technology-Hellas, P.O. Box 1527, 71110 Heraklio, Crete, Greece

Madhu Menon^{b)}

Department of Physics and Astronomy, University of Kentucky, Lexington, Kentucky 40506-0055 and Center for Computational Sciences, University of Kentucky, Lexington, Kentucky 40506-0045

Deepak Srivastava^{c)}

NASA Ames Research Center, CSC, Moffett Field, California 94035-1000

(Received 11 March 2002; accepted 14 May 2002)

We present an efficient transfer matrix formalism for obtaining the quantum conductivity of single-wall carbon nanotubes (SWCN's) based on a nonorthogonal tight-binding scheme. The formalism is used to calculate conductivity in the presence of topological defects and H adsorbates. *I-V* characteristics show large oscillatory behavior as a function of the number of H adatoms for both (10,0) and (5,5) SWCN's. Furthermore, the conductivity is found to depend sensitively on structural relaxation. © 2002 American Institute of Physics. [DOI: 10.1063/1.1491406]

I. INTRODUCTION

The unusual electronic properties of single-wall carbon nanotubes (SWCN's) show great promise in their potential for use in molecular electronic devices. The electronic structure of these tubes can be either metallic or semiconducting, depending on both the diameter and chirality which can be uniquely determined by the chiral vector (n,m) , where n and m are integers.¹ For practical application of their device properties, a full characterization of electronic behavior (*I-V* characteristics) is essential. The *I-V* characteristics, in turn, are sensitively dependent on the presence of defects (Stone–Wales,² vacancy, and substitutional) and adsorbates. An accurate numerical estimation of the transport quantities must, therefore, take all these factors into account in a realistic manner.

The effect of topological (pentagon-heptagon) defects on the transport properties of SWCN's have been the subject of several studies. The defects were found to cause a small increase in the electron density of states (DOS), at the Fermi level, E_F . This was attributed to the localized defect states acting as point scatterers in the electronic transmission.^{3,4} While Crespi *et al.*³ did not find any gap opening for (5,5) SWCN's due to the presence of defects, Anantram and Govindan⁵ predicted that the existence of ten strong isolated random scatterers on the wall of a (10,10) SWCN opens a transmission gap at E_F proportional to the defect density.

SWCN's containing topological defects are difficult to make in experiments in any controlled way. Experimentally it is much easier to incorporate adsorbates by exposure. Recent experiments suggest the electronic properties to have extreme sensitivity to chemical environment. In particular,

exposure to gaseous molecules such as oxygen, NO₂, or NH₃ results in orders of magnitude change in the electrical resistivity of semiconducting nanotubes.^{6,7} Changes in the resistivity of SWCN's were also observed resulting from adsorption of N₂, He, and H₂.⁸ Most of the works on the H interaction with SWCN's are focused on the description of the structural configuration around the H-SWCN bond and its energetics and their consequence in the possibilities for H storage offered by the nanotube.^{9–13} To the best of our knowledge, there is no work reported on the effect of H adsorption on the transport properties of SWCN's.

It is thus clear that the presence of defects and adsorbates on SWCN's provide an interesting opportunity to study their effects on conductivity. Results of the quantum conductivity calculations can be used as a guide in tailoring the structures to realize useful device applications of these materials.

The quantum conductivity of SWCN's has been investigated theoretically by several groups using various methods. The most commonly used computational schemes for calculating the (coherent) current in a SWCN is based on the Landauer expression which relates the electron conductance G with the transmission function $T(E)$.¹⁴ The latter is usually obtained within either the transfer Hamiltonian approach^{15,16} or the Green's function scattering formalism.^{17,18} The Green's function approach coupled with a simple tight-binding (TB) model with one π electron per atom has been used by many groups to calculate the SWCN conductivity.^{18–20}

A common feature of all these methods is the use of TB formalism to obtain conductivity. The popularity of TB formalism for quantum conductivity calculations stems from the computational efficiency of the method which derives from the fact that the Hamiltonian can be parametrized. Furthermore, the electronic structure information can be easily ex-

^{a)}Electronic mail: andriot@iesl.forth.gr

^{b)}Electronic mail: super250@pop.uky.edu

^{c)}Electronic mail: deepak@nas.nasa.gov

tracted from the TB Hamiltonian. A number of simplifying assumptions are usually made, however, to make these calculations more tractable. The most common assumption is to restrict the tight-binding Hamiltonian to only one π -electron orbital per atom. Furthermore, most of these calculations neglect the effects of structural relaxation altogether. Even while performing relaxation, most use classical many-body potentials. Use of tight-binding Hamiltonian for relaxation is very rare. Among the works on conductivity quoted above, only Refs. 3 and 12 report relaxation using quantum methods. Also, all of the TB calculations used so far for conductivity calculations make the assumption that the basis set is orthogonal. Nevertheless, most of these approaches are successful in elucidating many salient features of quantum conductivity of SWCN's.

Due to its simplicity, the transfer matrix method of Tsukada and Shima²¹ in the one π -orbital approximation has proved very useful in calculating scanning tunneling microscopy (STM) and scanning tunneling spectroscopy (STS) images of SWCN (Refs. 22 and 23) and in transport calculations.²⁴ However, Choi *et al.*²⁵ have demonstrated that *ab initio* results are sometimes quite different from the single one π -orbital TB calculations. This is especially true in small-diameter SWCN's where the hybridization of s and p orbitals of carbon gives rise to the splitting of π and π^* bands responsible for metallicity. This fact is being recognized by some groups working in the area of SWCN conductivity. For example, Rochefort *et al.*²⁶ have applied the extended Huckel method with an emphasis on the coupling between the π - and σ -electron states for bent SWCN's. It should also be noted that one π -orbital approximation results in symmetric variation of the DOS and conductance with respect to the Fermi energy (see, for example, Fig. 3 of Ref. 27) while the sp^3 parametrization does not. This symmetry is persistent even in the presence of point defects (see Fig. 2 of Ref. 28). In view of these results, we believe that one π -orbital approximation is inadequate in the treatment of defects resulting from adsorption and the full sp^3 parametrization appears more appropriate.

The nonorthogonal TB schemes have been shown to give vastly improved results over orthogonal TB models for structural relaxation of silicon and carbon systems, especially when structural deformations are present.^{29,30} In particular, the nonorthogonal tight-binding molecular dynamics scheme of Menon and Subbaswamy has been used successfully to study C and Si systems ranging from small clusters to bulk solids.^{29,30} A quantum conductivity formalism for SWCN's making use of the nonorthogonal TB Hamiltonian incorporating full sp^3 parametrization is, therefore, timely and desirable. This enables us to make use of the *same* Hamiltonian for calculating quantum conductivity as well as for performing structural relaxation.

Recently, a number of *ab initio* transport calculations have been reported based on the density functional theory (DFT).³¹⁻³³ Although the applications of these methods were limited to systems consisting of a small number of atoms and/or to systems limited to s - p configurations, these methods are very valuable in providing a useful test for more widely used semiempirical methods including the present

one. It should be noted, however, that the DFT-based methods cannot match the advantages offered by the semiempirical methods for obtaining both lattice relaxation and transport properties on the same footing in realistic systems.

In the next section, we present a transfer Hamiltonian approach for calculating quantum conductivity of SWCN based on the nonorthogonal TB scheme of Menon and Subbaswamy. The conductivity is obtained for pristine SWCN's as well as in the presence of topological defects and adsorbates. The conductance is found to depend sensitively on these.

II. THEORY

The most commonly used computational schemes for calculating the (coherent) conductance Γ are the transfer Hamiltonian approach and the Green's function formalism.^{14-16,21,34-36} In these formalisms the tube conductance Γ of any sample (metallic or semiconducting) is written in terms of the transmission function T :

$$\Gamma = \frac{2e^2}{h} T. \tag{1}$$

Equation (1) is valid in the limit of a weak bias (linear response theory) and is equivalent to the Kubo formula.¹⁴ The frequency-dependent Kubo formula in the zero-temperature limit is more convenient as a starting expression from a calculational point of view and has the following expression:

$$\begin{aligned} \Gamma(\omega) = & \frac{2\pi e^2}{\omega \hbar^2} \int dE \sum_{n,m} |\langle n|J|m\rangle|^2 \\ & \times \delta(E - eV - E_m) \delta(E - E_n) \lim_{T \rightarrow 0} f(E) \\ & \times [1 - f(E + \hbar\omega)], \end{aligned} \tag{2}$$

where ω is the frequency, J the current operator, $f(E)$ the Fermi function, V the applied voltage, and $|n\rangle$, $|m\rangle$, E_n , and E_m denote the single electron states and their corresponding eigenvalues (see, for example, Ref. 37). In Eq. (2), it is implicitly assumed that the model Hamiltonian employed satisfies the *separability property*.¹⁶ Therefore, following Bardeen,¹⁵ we can write the tunneling matrix elements in terms of the matrix elements $J_{nm} = \langle n|J|m\rangle$ of the current operator. The latter are approximated in terms of the wave functions $\Psi_n(\mathbf{r}) \equiv |n\rangle$ according to the following equation:

$$J_{nm} = \frac{\hbar^2}{2m} \int d\mathbf{S} \cdot (\Psi_n^* \nabla \Psi_m - \Psi_m \nabla \Psi_n^*). \tag{3}$$

In the zero-frequency limit, Eq. (2) takes the form

$$\begin{aligned} \Gamma(\omega=0) = & \frac{I}{V} \\ = & \frac{2\pi e}{\hbar V} \sum_{n,m} |\langle n|J|m\rangle|^2 \lim_{T \rightarrow 0} f(E_n) \\ & \times [1 - f(E_m - eV)] \delta(E_n - E_m). \end{aligned} \tag{4}$$

By taking the zero-temperature limit for small V , Eq. (4) reduces to the following expression for the net current:

$$\Gamma_0 = \Gamma(\omega=0, T=0)$$

$$= \frac{I}{V} = \frac{2\pi e^2}{\hbar} \sum_{nm} |\langle n|J|m\rangle|^2 \delta(E_n - E_F) \delta(E_m - E_F), \quad (5)$$

where E_F is the Fermi energy.

Equation (5) should be recognized as the expression for the tunneling conductance as obtained by first-order perturbation theory¹⁵ and the transfer Hamiltonian approach (THA).¹⁶ In the latter case, the single-electron states $|n\rangle$ and $|m\rangle$ correspond, respectively, to the states of the left (to be denoted by L) and right (to be denoted by R) leads of the conducting tube.

Tight-binding approximation to the transfer Hamiltonian approach

The transfer Hamiltonian approach [as described by Eqs. (4) and (5)] and the Green's function approach represent the starting points for two of the most commonly used computational schemes for the calculation of tunneling currents. While there are advantages and disadvantages to both in implementing approximations for practical use, the computational efficiency of both schemes can be greatly improved by using the TB approximation.

In order to incorporate the TB approximation in the formalism described by Eq. (4), we follow the works of Tsukada and Shima²¹ by generalizing their treatment to cases in which more than one atomic orbitals are present. We write the single-electron wave functions $\Psi_n(\mathbf{r})$ as a superposition of atomic orbitals $\phi_\alpha(\mathbf{r}-\mathbf{R}_i)$ of type $\alpha = s, p_x, p_y, p_z, d_{xy}, \dots$, located at every equivalent lattice site specified by the position vectors \mathbf{R}_i , i.e.,

$$\Psi_n^\Lambda(\mathbf{r}) = \sum_{i\alpha} c_{i\alpha n}^\Lambda \phi(\mathbf{r}-\mathbf{R}_i), \quad \Lambda = L, R, \quad (6)$$

where the indices L and R indicate that the labeled quantities refer to the left and right leads, respectively, and $c_{i\alpha n}^\Lambda$ are constants to be determined. By substituting Eq. (6) into Eq. (5) and following Ref. 21, Eq. (5) can be rewritten in the TB approximation as

$$I = 2\pi e\hbar \int dE \{f(E) - f(E - eV)\} \times \sum_{ii'\alpha\alpha'} \sum_{jj'\beta\beta'} G_{L,ii'}^{*\alpha\alpha'}(E) G_{R,jj'}^{\beta\beta'}(E) J_{ij}^{*\alpha\beta} J_{i'j'}^{\alpha'\beta'}, \quad (7)$$

where (see also Ref. 36)

$$G_{\Lambda,ii'}^{\alpha\alpha'} = \sum_n c_{ian}^{*\Lambda} c_{i'\alpha'n}^\Lambda \delta(E - E_n), \quad \Lambda = L, R, \quad (8)$$

and

$$J_{ij}^{\alpha\beta} \equiv \int_S d\mathbf{S} \cdot \mathbf{j}_{ij}^{\alpha\beta}, \quad (9)$$

with

$$\mathbf{j}_{ij}^{\alpha\beta} = \frac{\hbar}{2m} \{ \phi_\alpha^{*L}(\mathbf{r}-\mathbf{R}_i) \nabla \phi_\beta^{*R}(\mathbf{r}-\mathbf{R}_j) - \phi_\beta^{*R}(\mathbf{r}-\mathbf{R}_j) \nabla \phi_\alpha^L(\mathbf{r}-\mathbf{R}_i) \}. \quad (10)$$

The computation of the tunneling current given by Eqs. (7)–(10) can be expedited if the surface integral of Eq. (9) can be written as a volume integral.²¹ The current matrix elements can then be expressed as

$$J_{ij}^{\alpha\beta} = \frac{1}{\hbar} \int \phi_\alpha^{*L}(\mathbf{r}-\mathbf{R}_i) \{V_L(\mathbf{r}) - V_R(\mathbf{r})\} \times \phi_\beta^R(\mathbf{r}-\mathbf{R}_j) d\mathbf{r}, \quad (11)$$

where $V_\Lambda(\mathbf{r})$, $\Lambda = L, R$, denotes the single-electron potential of the $\Lambda = L, R$ metallic lead.

Evaluation of $J_{ij}^{\alpha\beta}$ can be further simplified when one notes that within the TB approximation the current matrix elements $J_{ij}^{\alpha\beta}$ have nonvanishing contribution only when i and j are nearest neighbors. Equation (11) can then be approximated as follows:

$$J_{ij}^{\alpha\beta} \approx \frac{\langle V_L(\mathbf{r}) - V_R(\mathbf{r}) \rangle_{ij}}{\hbar} \int \phi_\alpha^{*L}(\mathbf{r}-\mathbf{R}_i) \phi_\beta^R(\mathbf{r}-\mathbf{R}_j) d\mathbf{r} \quad (12)$$

or

$$J_{ij}^{\alpha\beta} \approx \frac{1}{\hbar} V_{ij} S_{ij}^{\alpha\beta}, \quad (13)$$

where $S_{ij}^{\alpha\beta}$ are the overlap matrix elements and the single-electron potential $V_{ij} = \langle V_L(\mathbf{r}) - V_R(\mathbf{r}) \rangle_{ij}$ is approximated as follows:

$$V_{ij} = \langle V_L(\mathbf{r}) - V_R(\mathbf{r}) \rangle_{ij} = \begin{cases} 0, & z \leq z_L, \\ V, & z \geq z_R, \\ \frac{V}{2} \left(\frac{z_i - z_L}{z_R - z_L} + \frac{z_j - z_L}{z_R - z_L} \right), & z_L \leq z, z_i, z_j \leq z_R, \end{cases} \quad (14)$$

where $\mathbf{r} = (x, y, z)$ is the position vector and it has been assumed that the tube axis is along the z axis and the lead terminals make contact with the tube across the planes $z = z_L$ and $z = z_R$ with $z_L < z_R$. The variables z_i and z_j are the z components of the position vectors \mathbf{R}_i and \mathbf{R}_j , respec-

tively. Inherent in the approximation made in Eq. (14) is the assumption of featureless contact between the electrodes and the tube. No contact details are introduced as done in the case of the surface Green's function matching method,¹⁸ which is in extensive use.

In terms of the approximations described by Eqs. (12)–(14), the expression for the tunneling current given by Eq. (7) now takes the form

$$I = \frac{\pi e}{2\hbar} \int_{E_F - eV}^{E_F} dE \{f(E) - f(E - eV)\} \\ \times \sum_{ii'\alpha\alpha'} \sum_{jj'\beta\beta'} G_{L,ii'}^{*\alpha\alpha'}(E) G_{R,jj'}^{\beta\beta'}(E - eV) \\ \times V_{ij} V_{i'j'} S_{ij}^{\alpha\beta} S_{i'j'}^{\alpha'\beta'}. \quad (15)$$

Equation (7) has been shown to describe the tunneling current in SWCN junctions reasonably well.³⁴ In the case of SWCN's, the wave functions ϕ_α^L and ϕ_β^R are the eigenfunctions of one single system representing the tube and junction. Therefore, these wave functions can be obtained by solving the corresponding Schrödinger equation (of the tube with the junction) in the nonorthogonal TB approximation. [This implies that the separability property is satisfied in order to allow one to make use of Bardeen's approximation,¹⁵ i.e., Eqs. (2) and (3).] We make use of the TB scheme proposed by Menon and Subbaswamy^{29,30} to obtain the overlap matrix elements, $S_{ij}^{\alpha\beta}$, in Eq. (15). This method has the advantage that both S_{ij} and the wave functions can be obtained from a single calculation. The TB parameters used for C are taken from Ref. 29. For the TB description of H and C-H interactions, we use the generalization of the nonorthogonal formalism to heteroatoms.³⁸ The parameters used for H (using the notation of Table I of Ref. 38) are $\epsilon_s = -13.6$, $r_0 = 0.35$, $K_0 = 3.7$, $\chi_0 = 5.37$, and $\sigma = 14.5$. Also, as in Ref. 38, the distance dependence of the interactions is exponential.

The present approach thus allows us to use the *same* Hamiltonian to calculate quantum conductivity as well as perform structural relaxation. As will be shown in Sec. III, the present formalism appears to be very promising in the calculation of tunneling currents in the SWCN's.

III. RESULTS

In this section we present the results obtained by the application of the transfer matrix formalism in various cases. They include *I-V* characteristics for a pristine SWCN as well as in the presence of topological defects and hydrogen adsorption. Our system consists of finite-length (10,0) and (5,5) SWCN's containing 164 and 150 C atoms, respectively, when no adsorbates are present. Each tube is capped at both ends to avoid dangling bond effects that may interfere with the defect and adsorbate induced states. Most previous theoretical works on quantum conductivity have primarily dealt with infinite length nanotubes on account of the simplification offered in the formalism. Experimental works, however, have provided evidence for transport through finite length nanotubes.^{39–41} In particular, Orlikowski *et al.*²⁷ have carried out quantum transport calculations of finite-length SWCN's using a single-band π -orbital TB model. They also repeated their conductivity calculations using a four-orbital *s,p* tight-binding model proposed by Charlier *et al.*,⁴² although structural relaxations were performed using classical many-body

potentials. The Hamiltonian used in both these models was taken to be orthogonal. Also, no *I-V* characteristics were given for the systems considered.

Prior to obtaining the conductivity we relax all structures without any symmetry constraints using the nonorthogonal tight-binding molecular dynamics scheme of Menon and Subbaswamy.^{29,30} The interactions between atoms in this model are not restricted to nearest neighbors and includes farther neighbors. Quantum conductivity calculations are then performed using the transfer matrix formalism outlined in Sec. II, which makes use of the *same* nonorthogonal tight-binding Hamiltonian. Use of the same Hamiltonian for calculating conductivity as well as the structural relaxation, thus, ensures a consistent approach. The *I-V* characteristics for all the systems considered are obtained using Eq. (15) in Sec. II.

A. Defects

Even though ideal carbon nanotubes consist of rolled up hexagonal graphene sheet, the presence of topological defects cannot be completely avoided under experimental conditions for producing these tubes. These include carbon rings in the form of pentagons, heptagons, octagons, and even squares. The presence of a pentagon-heptagon pair of defects is necessary for connecting two dissimilar nanotubes.^{28,43} Furthermore, three-point junctions require an excess of heptagons over pentagons in accordance with Euler's theorem for a closed structure.^{43,44}

By rotating a C—C bond in a simple nanotube by 90° one can create two pairs of adjacent pentagon-heptagon defects (7-5-5-7 Stone–Wales defect²) in an otherwise perfect hexagonal arrangement of carbon atoms. In Fig. 1 we show fully relaxed geometries of (10,0) and (5,5) SWCN's containing such defects.

To determine the strength of scattering from a single defect center in (10,0) and (5,5) SWCN's, we compute the *I-V* characteristics on tubes with single Stone–Wales (SW) defects. In one case the SW defect is aligned along the tube axis and in the other case perpendicular to the tube axis (Fig. 1). In Fig. 2 we show *I-V* curves for the (10,0) and (5,5) nanotubes in the presence of SW defects and compare the results with the defect-free cases. As seen in the figure, there is an enhancement in the current for larger voltages due to the presence of defects.

The current enhancements due to the presence of topological defects can be better understood by studying the behavior of the density of states⁴⁵ in the vicinity of the Fermi energy E_F , shown in Fig. 3. As seen in the DOS figure, additional peaks are introduced in the gap as a result of the defects when compared to the pristine SWCN case.

The increase in the DOS near E_F is in agreement with the results of Ref. 3. The reduction of some resonance DOS peaks while the appearance of new resonance peaks obtained in our calculations is also in agreement with other reported works.^{24,27,28} We also do not find any gap opening due to the presence of the defects.

To investigate the effect of SW defects on the symmetry in the conductance we plot the *I-V* characteristics in the full range. The results for both (10,0) and (5,5) SWCN's are

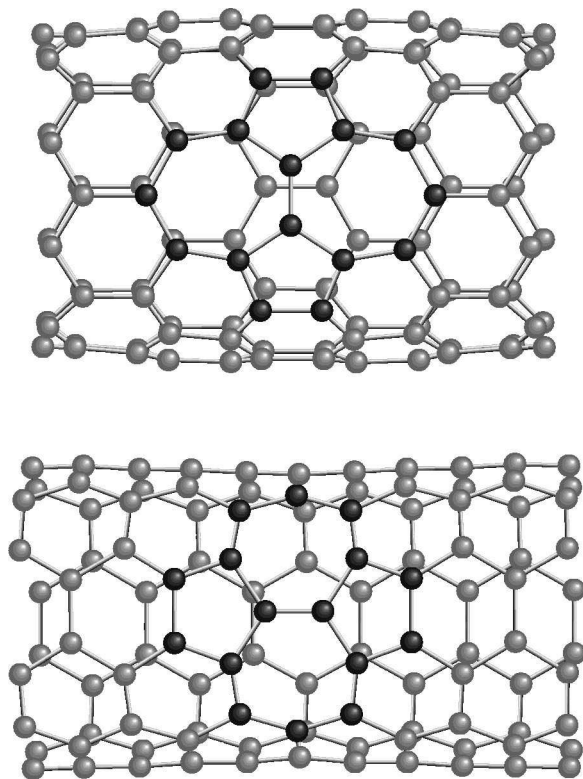


FIG. 1. Fully relaxed geometries of (10,0) and (5,5) SWCN's containing two pairs of pentagon-heptagon defects each. The defects were created by rotating C—C bonds of the SWCN by 90° .

shown in Fig. 4. As can be seen in the figure, in both cases, a slight asymmetry is observed in the I - V characteristics indicating that the randomly placed isolated defects within nanotube are very weak scattering centers of the current flowing through the system. As a result, they may not have significant effects from device applications perspective. It is worth noting that in the single-band π -orbital calculations of Harigaya,⁵¹ the DOS of a (5,5) and a (10,10) SWCN both

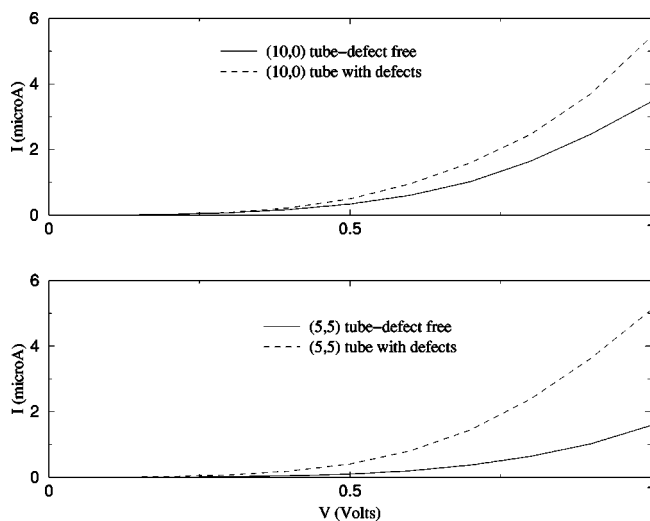


FIG. 2. Current versus voltage characteristics for the (10,0) (top panel) and (5,5) (bottom panel) nanotubes in the presence of two pairs of adjacent pentagon-heptagon defects shown in Fig. 1. The presence of defects seems to enhance the current in both types of nanotubes.

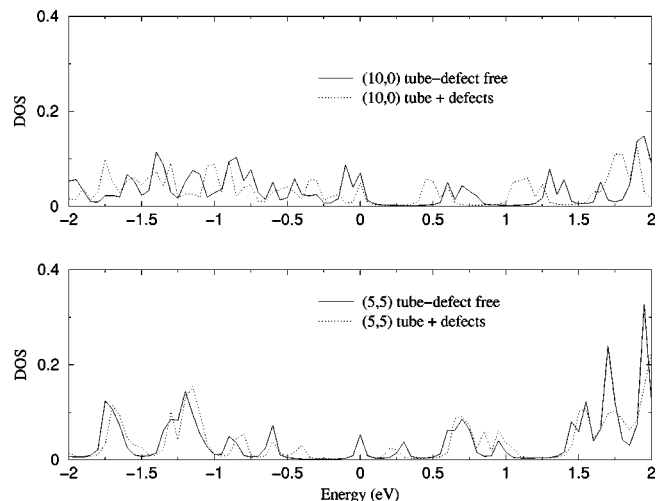


FIG. 3. Density of states (DOS) in the vicinity of the Fermi energy E_F . The Fermi energy is at 0 eV. As seen in the figure, additional peaks are introduced in the gap as a result of the defects when compared to the pristine SWCN case.

with bond and site disorder appears symmetric with respect to E_F . The appearance of such symmetry may be an inherent feature of the π -orbital approximation.

B. Hydrogen adsorption

The nature of the atomic H interaction with SWCN's and, in particular, the question whether as to H physisorbs or chemisorbs on SWCN's are an issue of current scientific debate. Equally uncertain is the case of the H_2 interaction with SWCN's. Recently, Froudakis⁴⁶ using a mixed quantum mechanics/molecular mechanics (QM/MM) model within the ONIOM method investigated the interaction of a (4,4) tube with H and showed that H binds in zigzag rings around the tube walls resulting in a considerable tube relaxation which increases the tube volume. Within the ONIOM method Bauschlicher⁴⁷ finds the binding energy (BE) of H on an atop position of a (10,0) SWCN to be 21.6 kcal/mol (0.94 eV), a

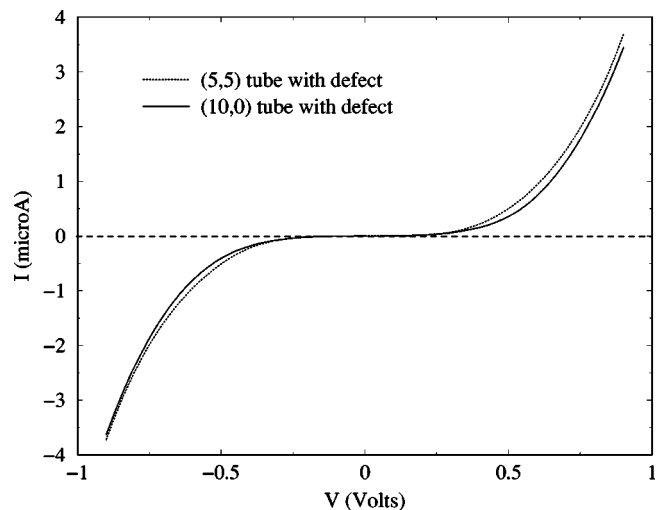


FIG. 4. The I - V characteristics for (10,0) and (5,5) SWCN's with single Stone-Wales defects in the full range showing slight asymmetry.

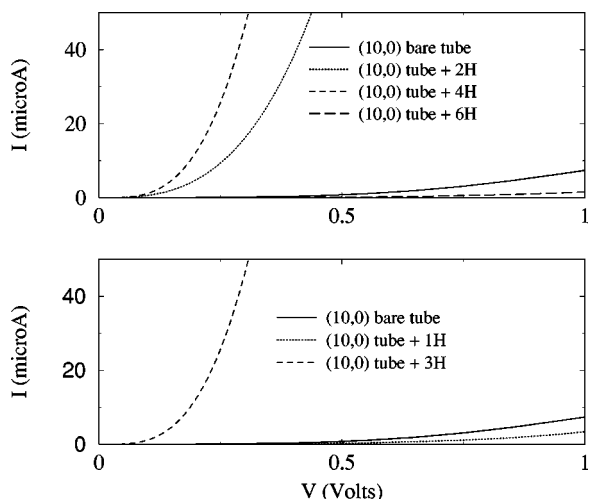


FIG. 5. The I - V curves for a semiconducting (10,0) nanotube with up to six adsorbed H atoms. The top panel includes results for even number of H, while the bottom panel contains results for odd number of H atoms. Large oscillations seen indicate extreme sensitivity to H adsorption.

value much smaller than that found by Froudakis (2.5 eV). This difference may point to the strong influence of tube chirality on H adsorption. We also note that in a recent article, Gulseren *et al.*¹³ obtain a BE value for H adsorption on (8,0) nanotube to be slightly larger than 2 eV. This is in good agreement with 1.98 eV reported by us.⁴⁸ Also, as stated in Sec. I, currently no work is reported on the effect of H adsorption on the transport properties of SWCN's.

In this section we present our results from the study of the effects of H adsorption on the transport properties of SWCN's by calculating I - V curves for both bare and H adsorbed (5,5) and (10,0) tubes. Our system consists of finite-length (5,5) and (10,0) SWCN's containing 150 and 164 C atoms, respectively. As indicated earlier, tubes are capped at both ends to avoid the influence of dangling bond effects. The H-adsorbed SWCN systems investigated consisted of up to six H atoms on SWCN. In all cases a fully symmetry unconstrained relaxation is performed using the nonorthogonal tight-binding molecular dynamics scheme of Menon and Subbaswamy.

The current versus voltage characteristics for a semiconducting (10,0) and a metallic (5,5) nanotube as a function of H coverage is shown in Figs. 5 and 6, respectively. The H coverage is varied from about 1/164 to 6/164 for the (10,0) nanotube and about 1/150 to 6/150 for the (5,5) nanotube. The hydrogen adsorbed nanotube is fully relaxed without any symmetry constraints in each case before conductivity calculations are performed. As seen in Figs. 5 and 6, the current as a function of voltage for a fixed H coverage increases monotonically up to 1.0 V without any sign of saturation as a function of voltage within the range calculated with our method. The I - V characteristics of both the metallic (5,5) and semiconducting (10,0) nanotubes show rather large oscillations as a function of H coverage, showing extreme sensitivity to H adsorption.

In both cases, as the coverage is increased from randomly placed one H atom to six H atoms, the current first increases for up to three randomly placed H atoms on the

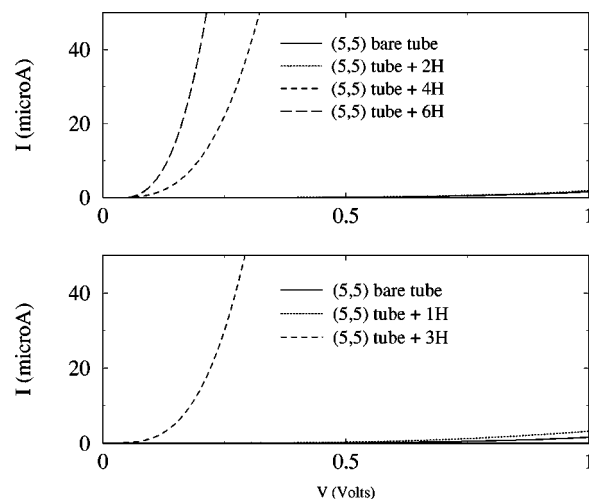


FIG. 6. The I - V curves for a metallic (5,5) nanotube with up to six adsorbed H atoms, also showing extreme sensitivity to H adsorption.

nanotubes and then starts to decrease at four H atoms on the nanotube for all bias voltages used. For the (10,0) nanotube decrease in the current continues also to the coverage of six H atoms where the curve almost overlaps the curve for the initial starting curve for only one H atom on the nanotube considered. In the (5,5) nanotube the decrease in the current observed between three and four H atoms chemisorption cases does not continue. The current for six H atoms chemisorption case starts to show an increase again. It seems, from the above observations, that the oscillations in the I - V characteristics as a function of the H coverage in the (10,0) nanotube have reached their peak within the H coverage range covered in this work. The I - V characteristics of the metallic tube also show a peaking behavior between three and four H chemisorption cases, but the current increases to larger values for the six H chemisorption case.

The oscillating features found here is qualitatively similar to that found for the same system treated using a Green's function embedding approach making use of the formalism introduced by Datta¹⁸ to obtain conductivity from the transmission function.⁴⁸ It therefore appears that the model approximations in the present work that assume a linear potential drop along the tube do not affect the basic conclusions arrived at using the Green's function approach where the potential drop is assumed to take place at the tube-lead interfaces and is symmetrically distributed between the two contacts.⁴⁸ Interestingly, recent experimental works have found that exposure to gaseous molecules such as oxygen, NO₂, or NH₃ results in orders of magnitude change in the electrical resistivity of semiconducting nanotubes.^{6,7} Some small-band-gap semiconducting nanotubes were even observed to become metallic upon oxygen dosing.⁶ Furthermore, while exposure to NO₂ molecules increased the conductance of the SWCN sample by about three orders of magnitude, conductance of the SWCN sample was observed to decrease \approx 100-fold after exposure to NH₃.

In Fig. 7, we show the calculated DOS for different H coverages on the (10,0) nanotube. In all cases the systems were fully relaxed using the nonorthogonal TB molecular

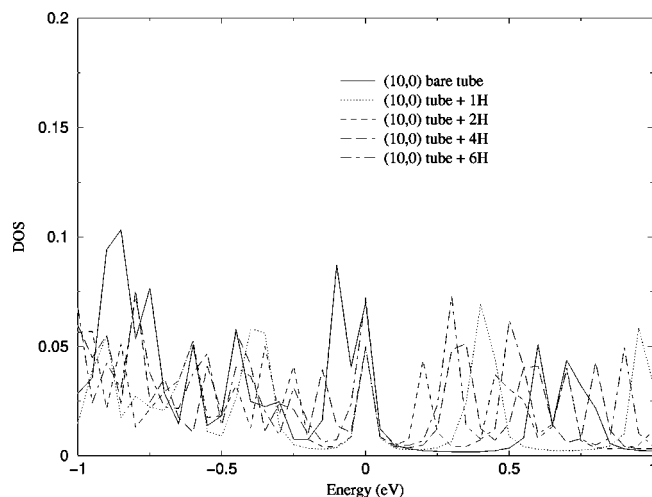


FIG. 7. Density of states (DOS) in the vicinity of the Fermi energy E_F for different H coverage for a (10,0) tube. The Fermi energy is at 0 eV. As seen in the figure, additional peaks are introduced in the gap as H coverage is increased.

dynamics. A careful observation reveals oscillations in the highest occupied molecular orbital (HOMO) and lowest unoccupied molecular orbital (LUMO) gap as the number of H adsorbates increase. Similar oscillatory behavior of the HOMO-LUMO gap for H adsorption was also obtained using *ab initio* calculations in our earlier work.⁴⁸

It should be noted that our manner of adding the H atoms to the nanotubes for conductivity calculations is completely random, the only restriction being that hydrogens are sufficiently far away from each other, preventing any interaction among themselves. This study is quite analogous to that reported by Hansson *et al.*,⁴⁹ who studied the effect of vacancies on the transport properties of finite-size SWCN. As is apparent from Fig. 5 of Hansson *et al.*,⁴⁹ the effect of vacancies is not monotonic (with the vacancy concentration) for small defect concentrations. Instead, the current can increase or decrease depending on the number of defects and their distribution on a (5,5) nanotube wall in complete analogy with the present case of defects due to H adsorption. As will be shown in Sec. III C, this effect of the point defects may become significant as a result of lattice relaxation. From these studies one can conclude that a particular point defect (vacancy or adsorbed atom) distribution can cause strong or weak scattering depending on the structure of the wave function⁴⁹. A change in this distribution might change the scattering dramatically. As Hansson *et al.*⁴⁹ observe, the effect of point defects in finite-size SWCN's appears much smaller than in the case of infinite-length tubes due to the scattering dominated by the contact regions. Increasing the defect concentration leads to the defect contribution to the scattering becoming more noticeable.

It is worth noting that the absence of monotonic behavior is also found in the dependence of the electronic gap and the transport properties on the tube length of finite-size SWCN's.²⁷ In particular Orlikowski *et al.*²⁷ found that the gap in the electronic eigenvalue spectrum oscillates as the tube length increases. This was attributed (in the case of weak coupling of the tube to the metal leads) to the change

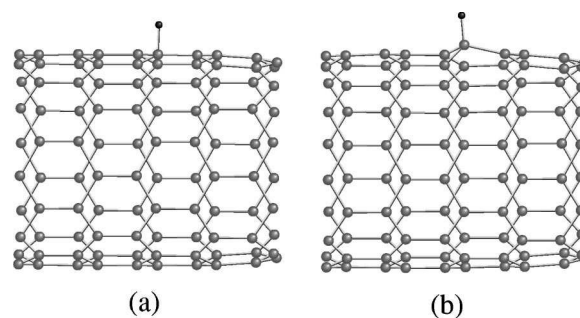


FIG. 8. The (a) unrelaxed and (b) relaxed configurations of a single H atom adsorbed on a (10,0) SWCN. As seen in the figure, the H chemisorption results in the underlying carbon atoms going from a planar (sp^2 type) to a pyramidal (sp^3 type) configuration.

in the number and distribution of the conduction resonance peaks as the tube length varies. This, in turn, and in view of the above discussion, can be attributed to the scattering conditions imposed on the wave functions by the different boundary conditions applied when the tube length is varied. Similar behavior was also reported in the case of carbon chains of various lengths.⁵⁰ All these make clear that the scattering details of low-dimension carbon systems (like carbon chains and SWCN's) are very sensitive to both their geometric details as well as the degree of their purity with respect to point defects and doping. We attribute this sensitivity, on the one hand, to the breaking of the conjugate-molecule picture (single-double bond alternation of the carbon bonds) by the point defects and, on the other hand, to the kind of the bond (single or double) involved in the contact to the electrodes.

C. Relaxation effects

In this section we study the effects of structural relaxation on the I - V characteristics. This effect is usually completely ignored in most quantum conductivity calculations.

In Figs. 8(a) and 8(b) we show the unrelaxed and relaxed configuration, respectively, of a single H atom adsorbed on a (10,0) SWCN. As seen in the figure, the H chemisorption results in the underlying carbon atoms going from a planar [sp^2 type, Fig. 8(a)] to a pyramidal [sp^3 type, Fig. 8(b)] configuration. The calculated I - V characteristics in the two cases are shown in Fig. 9. Even though the relaxation is local (Fig. 8), there is a significant difference in the values of the currents between the two cases. Structural relaxation can give rise to gap openings with simultaneous appearance of new defect states that can have significant effect on conductivity.²⁸

D. Summary

We have presented an efficient transfer matrix formalism for obtaining the quantum conductivity of SWCN's that makes explicit use of the nonorthogonality of the basis functions within the tight-binding scheme. The formalism allows us to perform symmetry unconstrained structural relaxation using the same Hamiltonian as used in the conductivity calculations. Current versus voltage characteristics of SWCN's have been obtained in the presence of topological defects as

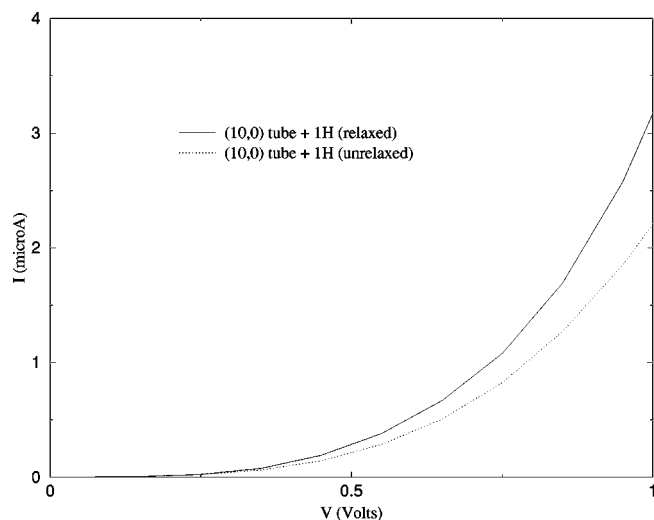


FIG. 9. The I - V curves for a semiconducting (10,0) nanotube with one adsorbed H atom (Fig. 6), showing the effects of structural relaxation.

well as when H adsorbates are present. I - V characteristics show large oscillatory behavior as a function of the number of H adatoms for both (10,0) and (5,5) SWCN's.

As stated earlier, the present results obtained within the transfer Hamiltonian approximation are in qualitative and quantitative agreement with those obtained⁴⁸ by us for a SWCN in contact with Ni leads using the surface Green's function matching (SGFM) method and Landauer's¹⁴ formalism for transport. Thus it appears that despite their "philosophical" differences, these two formalisms lead to the same conclusions. This should not be surprising if one recalls that the Ni-tube contact is weak and in this limit the THA has been shown to be the weak-coupling version of the scattering formalism as employed in the SGFM-Landauer formalism (see, for example, Ref. 18, pp. 161–163).

ACKNOWLEDGMENTS

The present work is supported through NSF Grant No. NER-0165121, MRSEC Program under Award No. DMR-9809686, DOE Grant No. 00-63857, NASA Grant No. 02-465679, and the University of Kentucky Center for Computational Sciences.

- ¹R. Saito, M. Fujita, G. Dresselhaus, and M. S. Dresselhaus, *Phys. Rev. B* **46**, 1804 (1992).
- ²A. J. Stone and D. J. Wales, *Chem. Phys. Lett.* **128**, 501 (1986).
- ³V. H. Crespi, M. L. Cohen, and A. Rubio, *Phys. Rev. Lett.* **79**, 2093 (1997).
- ⁴M. B. Nardelli and J. Bernholc, *Phys. Rev. B* **60**, R16 338 (1999).
- ⁵M. P. Anantram and T. R. Govindan, *Phys. Rev. B* **58**, 4882 (1998).
- ⁶P. C. Collins, K. Bradley, M. Ishigami, and A. Zettl, *Science* **287**, 1801 (2000).
- ⁷J. Kong, N. R. Franklin, C. Zhou, M. G. Chapline, S. Peng, K. Cho, and H. Dai, *Science* **287**, 622 (2000).
- ⁸G. U. Sumanasekera, C. K. W. Adu, S. Fang, and P. C. Eklund, *Phys. Rev. Lett.* **85**, 1096 (2000).
- ⁹Y. Ma, Y. Xia, M. Zhao, R. Wang, and L. Mei, *Phys. Rev. B* **63**, 115422 (2001).

- ¹⁰P. Dubot and P. Cenedese, *Phys. Rev. B* **63**, 241402 (2001).
- ¹¹K. Tada, S. Furuya, and K. Watanabe, *Phys. Rev. B* **63**, 155405 (2001).
- ¹²T. Yildirim, O. Gulseren, and S. Ciraci, *Phys. Rev. B* **64**, 075404 (2001).
- ¹³O. Gulseren, T. Yildirim, and S. Ciraci, *Phys. Rev. Lett.* **87**, 116802 (2001).
- ¹⁴R. Landauer, *Z. Phys. B: Condens. Matter* **68**, 217 (1987).
- ¹⁵J. Bardeen, *Phys. Rev. Lett.* **6**, 57 (1961).
- ¹⁶C. B. Duke, in *Solid State Physics*, edited by F. Seitz, D. Turnbull, and H. Ehrenreich (Academic, New York, 1969).
- ¹⁷D. S. Fisher and P. A. Lee, *Phys. Rev. B* **23**, 6851 (1981).
- ¹⁸S. Datta, in *Electronic Transport in Mesoscopic Systems* (Cambridge University Press, Cambridge, England, 1995).
- ¹⁹M. P. Samanta, W. Tian, S. Datta, J. I. Henderson, and C. P. Kubiak, *Phys. Rev. B* **53**, R7626 (1996).
- ²⁰M. B. Nardelli, *Phys. Rev. B* **60**, 7828 (1999).
- ²¹M. Tsukada and N. Shima, *J. Phys. Soc. Jpn.* **56**, 2875 (1987).
- ²²V. Meunier and Ph. Lambin, *Phys. Rev. Lett.* **81**, 5588 (1998).
- ²³V. Meunier, P. Senet, and Ph. Lambin, *Phys. Rev. B* **60**, 7792 (1999).
- ²⁴D. Orlikowski, M. B. Nardelli, J. Bernholc, and C. Roland, *Phys. Rev. B* **61**, 14 194 (2000).
- ²⁵H. J. Choi, J. Ihm, S. G. Louie, and M. L. Cohen, *Phys. Rev. Lett.* **84**, 2917 (2000).
- ²⁶A. Rochefort, P. Avouris, F. Lesage, and D. R. Salahub, *Phys. Rev. B* **60**, 13 824 (1999).
- ²⁷D. Orlikowski, H. Mehrez, J. Taylor, H. Guo, J. Wang, and C. Roland, *Phys. Rev. B* **63**, 155412 (2001).
- ²⁸L. Chico, V. H. Crespi, L. X. Benedict, S. G. Louie, and M. L. Cohen, *Phys. Rev. Lett.* **76**, 971 (1996).
- ²⁹M. Menon, E. Richter, and K. R. Subbaswamy, *J. Chem. Phys.* **104**, 5875 (1996).
- ³⁰M. Menon and K. R. Subbaswamy, *Phys. Rev. B* **55**, 9231 (1997).
- ³¹J. Taylor, H. Guo, and J. Wang, *Phys. Rev. B* **63**, 245407 (2001).
- ³²M. Brandbyge, J.-L. Mozos, P. Ordejon, J. Taylor, and K. Stokbro, *Phys. Rev. B* **65**, 165401 (2002).
- ³³M. B. Nardelli, J.-L. Fatterbert, and J. Bernholc, *Phys. Rev. B* **64**, 245423 (2001).
- ³⁴R. Saito, G. Dresselhaus, and M. S. Dresselhaus, *Phys. Rev. B* **53**, 2044 (1996).
- ³⁵C. M. Soukoulis and E. N. Economou, *Waves Random Media* **9**, 255 (1999).
- ³⁶For the physical meaning of $G_{\Lambda,ii}^{aa'}$, see V. Meunier *et al.*, *Phys. Rev. B* **60**, 7792 (1999).
- ³⁷J. Mathon, *Phys. Rev. B* **56**, 11 810 (1997).
- ³⁸M. Menon, *J. Chem. Phys.* **114**, 7731 (2001).
- ³⁹S. J. Tans, M. H. Devoret, H. Dai, A. Thess, R. E. Smalley, L. J. Geerligs, and C. Dekker, *Nature (London)* **386**, 474 (1997).
- ⁴⁰M. Bockrath, D. H. Cobden, P. L. McEuen, N. G. Chopra, A. Zettl, A. Thess, and R. E. Smalley, *Science* **275**, 1922 (1997).
- ⁴¹L. C. Venema, J. W. G. Wildoer, J. W. Janssen, S. J. Tans, H. L. J. T. Tuistra, L. P. Kouwenhoven, and C. Dekker, *Science* **283**, 52 (1999).
- ⁴²J. C. Charlier, Ph. Lambin, and T. W. Ebbesen, *Phys. Rev. B* **54**, R8377 (1996).
- ⁴³D. Srivastava, S. Saini, and M. Menon, in *Molecular Electronics: Science and Technology*, edited by A. Aviram and M. Ratner [Ann. N.Y. Acad. Sci. **852**, 178 (1998)].
- ⁴⁴M. Menon and D. Srivastava, *Phys. Rev. Lett.* **79**, 4453 (1997).
- ⁴⁵The electron DOS is obtained according to the formula $\rho(E) = A \sum_i \delta[(E - \epsilon_i)^2 + \delta^2]$, where A a normalization constant and $\delta = 0.2$ eV.
- ⁴⁶G. E. Froudakis, *NanoLetters*, **1**, 179 (2001).
- ⁴⁷C. W. Bauschlicher, Jr., *Chem. Phys. Lett.* **322**, 237 (2000).
- ⁴⁸A. N. Andriotis, M. Menon, D. Srivastava, and G. E. Froudakis, *Phys. Rev. B* **64**, 193401 (2001).
- ⁴⁹A. Hansson, M. Paulsson, and S. Stafstrom, *Phys. Rev. B* **62**, 7639 (2000).
- ⁵⁰B. Larade, J. Taylor, H. Mehrez, and H. Guo, *Phys. Rev. B* **64**, 075420 (2001).
- ⁵¹K. Harigaya, *Phys. Rev. B* **60**, 1452 (1999).